CLM - M 103

CLM - M 103

UKAEA RESEARCH GROUP

Memorandum

COMPUTER CALCULATION OF NATURAL CONVECTION WITH UNIFORM HEAT GENERATION IN THE LIQUID

J H ADLAM

CULHAM LABORATORY
Abingdon Oxfordshire

1975

CLM-M 103

COMPUTER CALCULATION OF NATURAL CONVECTION WITH UNIFORM HEAT GENERATION IN THE LIQUID

by

J H Adlam

ABSTRACT

Calculations have been made which can be compared with the previous experimental results of Ralph and Roberts[1] and of Wilkie and Fisher[2]. The simplifying assumption of two-dimensional flow has been made for the calculation. There is no significant difference between this calculation and the previous experimental results considered.

UKAEA Research Group
Culham Laboratory
Abingdon
Oxon OX14 3DB
UK

September 1975

CONTENTS

ILLUSTRATIONS

Figure

SYMBOLS AND NOMENCLATURE

Physical Quantities in MKS Units

b	Temperature coefficient for volume change of liquid.	$^{o}C^{-1}$
C_p	Specific heat at constant pressure of liquid.	$J.kg^{-1}\ ^{o}C^{-1}$
$\underline{g}$	Acceleration due to gravity vector.	$m.s^{-2}$
g	Acceleration due to gravity (absolute value).	$m.s^{-2}$
H	Rate of generation of heat per unit volume of liquid.	$J.\ s^{-1}\ m^{-3}$
k	Thermal conductivity of liquid.	$J.\ s^{-1}\ m^{-1}\ ^{o}C^{-1}$
L	Length characteristic of a configuration.	m
p	Pressure in liquid.	$N.\ m^{-2}$
t'	Time	S
T'	Temperature of liquid.	^{o}C
$\underline{u}'$	Velocity vector of liquid.	$m.\ s^{-1}$
x', y', z'	Cartesian coordinates.	m
μ	Viscosity of liquid.	$kg.\ m^{-1}\ s^{-1}$
π	Difference between pressure and equilibrium hydrostatic pressure in liquid.	$N.\ m^{-2}$
ρ	Density of liquid.	$kg.\ m^{-3}$
ρ_o	Density of liquid at $0^{o}C$	$kg.\ m^{-3}$
$\underline{\nabla}$	$\equiv \underline{i}_x \frac{\partial}{\partial x} + \underline{i}_y \frac{\partial}{\partial y} + \underline{i}_z \frac{\partial}{\partial z}$	
	Vector gradient operator	m^{-1}
ν	$= \frac{\mu}{\rho_o}$	$m^2\ s^{-1}$
τ	$= \frac{L^2}{\nu}$	s
θ	$= \frac{HL^2}{k}$	^{o}C

Physical Quantities in the Normalised Units of this Report

The quantities,

t, T, $\underline{u}$, x, y, z,

written primed above are now written unprimed.

u	x- component of velocity vector.
v	y- component of velocity vector.
$\underline{\omega}$	Vorticity vector.
ω	z- component of vorticity vector.
$\underline{\psi}$	Stream function vector.
ψ	z- component of stream function vector.

Dimensionless Quantities

Ra	Rayleigh number.
Pr	Prandtl number.
M_L	Heat transfer parameter.

Nomenclature for Computation

Δx	Mesh spacing)
Δt	Time-step length) Normalised Units
$T_{i,j}$, $\omega_{i,j}$, $\psi_{i,j}$	Values for the quantities T, ω, ψ at the mesh point $x = i\,\Delta x$, $y = j\,\Delta x$.
$T^{n}_{i,j}$, $\omega^{n}_{i,j}$	Values of $T_{i,j}$, $\omega_{i,j}$ at a stage numbered n in the calculation.
$\psi^{n}_{i,j}$	n^{th} approximation in the calculation of $\psi_{i,j}$.
I	Identity tensor.
A	Tensor as defined by equation (14).
B	Tensor as defined by equation (15).

C	Tensor as defined by equation (16).
ΔT_s	Root mean square change in T meaned over the channel cross section.
$\Delta \omega_s$	Root mean square change in ω meaned over the cross section.
$\epsilon \omega_s$	Root mean square error in ω meaned over the cross section.
$(W_T)_{i,j}$	Relative error in calculation of T at mesh point i,j.
$(W_\omega)_{i,j}$	Relative error in calculation of ω at mesh point i,j.
$Max(Ar)$	The maximum value of an array Ar.
$\overline{F}$	The mean value of F taken over the channel cross section.
$\int dS$	Surface integral.
$\int dV$	Volume integral.
R_L	A quantity defined in the condition (18) which sets the accuracy of the solution by the relaxation method.
S	Initial value of random vorticity at the mesh points.
X, X_c	Quantities controlling the accuracy of calculation.
α, β, P, Q, $(\omega_{av})_{i,j}$	As defined in the text.

1. INTRODUCTION

Natural convection in a liquid, where there is a uniform generation of heat throughout the volume, has been considered. The calculation is two-dimensional, but the fundamental equations of physics are solved. One purpose is to compare calculated results with the previously obtained experimental results of Ralph and Roberts[1] and those of Wilkie and Fisher[2].

The method used here is basically the same as that used by Jahn and Reineke[3]. These authors have used a method previously used by Crowley[4] to calculate the changes produced by convective motion. The accuracy of the calculation has been checked and a method for improving this accuracy for points in the neighbourhood of the boundary has been introduced. Automatic adjustment of the calculation time-step length has been tried, to run the program to a prescribed accuracy. The extent to which this program succeeded has been indicated.

2. FUNDAMENTAL EQUATIONS

Quantities x', y', z', t', $\underline{u}'$, T', w', ψ' and ∇' in MKS units are here written primed, in order that the quantities in the normalised units which are to be used, may be written unprimed.

The equations which have to be solved are the equation of motion for a liquid.

$$\rho\left(\frac{\partial \underline{u}'}{\partial t'} + \underline{u}' . \underline{\nabla}' \underline{u}'\right) = - \nabla' p + \mu (\underline{\nabla}')^2 \underline{u}' + \rho \underline{g} \quad , \tag{1}$$

and the heat conduction equation for a liquid,

$$\rho C_p \left(\frac{\partial T'}{\partial t'} + \underline{u}' . \underline{\nabla}' T'\right) = k (\underline{\nabla}')^2 T' + H \tag{2}$$

H is here the rate of generation of heat per unit volume, which is taken as uniform throughout the liquid. The liquid is assumed incompressible with temperature coefficient for volume change b; so that

$$\rho = \rho_o(1 - b\,T').$$

Further write

$$\underline{\nabla}\pi = \underline{\nabla} p - \rho_o \underline{g}$$

Hence equation (1) becomes

$$\rho\left(\frac{\partial \underline{u}'}{\partial t'} + \underline{u}' \cdot \underline{\nabla}' \underline{u}'\right) = -\underline{\nabla}\pi + \mu(\underline{\nabla}')^2 \underline{u}' - b\,\underline{g}\,\rho_o T' . \qquad (3)$$

Normalised (unprimed) units are now defined as follows

$$t = \frac{t'}{\tau}\ ,\quad \left.\begin{matrix} x \\ y \\ z \end{matrix}\right\} = \left.\begin{matrix} x' \\ y' \\ z' \end{matrix}\right\} / L\ ,\quad \underline{u} = \underline{u}' \cdot \frac{\tau}{L}\ ,\quad T = \frac{T'}{\theta}\ ,$$

where L is some dimension in a configuration

and $$\nu = \frac{\mu}{\rho_o}\ ,\quad \tau = \frac{L^2}{\nu}\ ,\quad \theta = \frac{HL^2}{k}$$

Neglecting $\rho - \rho_o$, compared with ρ, equations (3) and (2) become respectively equations (4) and (5)

$$\frac{\partial \underline{u}}{\partial t} + \underline{u} \cdot \underline{\nabla}\,\underline{u} = \nabla^2 \underline{u} - \frac{Ra}{Pr} T . \underline{i}_g - \frac{L^2}{\nu^2 \rho_o} \underline{\nabla}\pi \qquad (4)$$

$$\frac{\partial T}{\partial t} + \underline{u} \cdot \underline{\nabla}\, T = \frac{1}{Pr} \nabla^2 T + \frac{1}{Pr}\ . \qquad (5)$$

Ra (the Rayleigh number) and Pr (the Prandtl number) are given by

$$Ra = \frac{b\,g\,H\,L^{5}\,\rho_o\,C_p}{\nu\,k^2} \quad , \quad Pr = \frac{\mu\,C_p}{k} \quad ,$$

and $\underline{i}_g$ is the unit vector in the direction of gravity. Since the liquid is incompressible there is the further equation,

$$\mathrm{div}(\underline{u}) = o. \tag{6}$$

An appropriate solution of equation (6) is,

$$\underline{u} = \mathrm{Curl}\ \underline{\Psi}.$$

Further write $\underline{\omega} = \mathrm{Curl}\ \underline{u}$ where $\underline{\omega}$ is called the vorticity.

Then performing the curl operation on both sides of equation (4)

$$\frac{\partial \underline{\omega}}{\partial t} - \mathrm{curl}(\underline{u} \wedge \underline{\omega}) = - \mathrm{curl}\ \mathrm{curl}(\underline{\omega}) - \frac{Ra}{Pr}\,\mathrm{curl}(T\underline{i}_g) \tag{7}$$

and equation (6) becomes

$$\underline{\omega} = \mathrm{curl}\ \mathrm{curl}\ \underline{\Psi} \ . \tag{8}$$

This calculation is concerned only with the two-dimensional case with Cartesian coordinates,

$$\underline{u} = u\,(x,y).\ \underline{i}_x + v\,(x,y).\ \underline{i}_y$$

$$\underline{\omega} = \omega\,(x,y).\ \underline{i}_z$$

$$\underline{i}_g = \underline{i}_y \ .$$

Equations (7) and (8) then become respectively the equations (9) and (10),

$$\frac{\partial \omega}{\partial t} + u\,\frac{\partial \omega}{\partial x} + v\,\frac{\partial \omega}{\partial y} = \frac{\partial^2 \omega}{\partial x^2} + \frac{\partial^2 \omega}{\partial y^2} - \frac{Ra}{Pr}\,\frac{\partial T}{\partial x} \tag{9}$$

$$\frac{\partial^2 \psi}{\partial x^2} + \frac{\partial^2 \psi}{\partial y^2} = -\omega \qquad (10)$$

Further equation (5) becomes,

$$\frac{\partial T}{\partial t} + u \frac{\partial T}{\partial x} + v \frac{\partial T}{\partial y} = \frac{1}{Pr} \left\{ \frac{\partial^2 T}{\partial x^2} + \frac{\partial^2 T}{\partial y^2} + 1 \right\} \qquad (11)$$

3. Time Advancing of the Vorticity (ω) and the Temperature (T)

Equation (9) of the previous section may be transposed so that $\frac{\partial \omega}{\partial t}$ is equal to the sum of a convective term $\left(- u \frac{\partial \omega}{\partial x} - v \frac{\partial \omega}{\partial y} \right)$ a diffusive term $\left(\frac{\partial^2 \omega}{\partial x^2} + \frac{\partial^2 \omega}{dy^2} \right)$ and a temperature gradient term $- \frac{Ra}{Pr} \frac{\partial T}{\partial x}$.

Similarly equation (11) may be transposed so that $\frac{\partial T}{\partial t}$ is the sum of a convective term $\left(- u \frac{\partial T}{\partial x} - v \frac{\partial T}{\partial y} \right)$ a diffusive term $\frac{1}{Pr} \left(\frac{\partial^2 T}{\partial x^2} + \frac{\partial^2 T}{\partial y^2} \right)$ and a heat generation term $\frac{1}{Pr}$. The quantities $\omega(x,y)$ and $T(x,y)$ are calculated on a rectangular mesh of points $\omega_{i,j}$ and $T_{i,j}$ over the cross section considered.

Considering both the vorticity ω and the temperature T, for all points except those close to the boundary the convective terms are larger than the other two; consequently errors in the convective terms have most effect on the accuracy of the calculation. The fourth order method described by Crowley was used to calculate the changes produced by the convective term. Crowley has shown that for the case where there is only a convective term (the colour equation) this method was much more accurate than a second order method. The diffusive term was calculated by a second-order method, as has been described by Jahn and Reineke, who also used Crowley's fourth order method for calculating the convective term. The calculation is carried out in three stages, with $f^{o}_{i,j}$

used to represent the initial value of either $\omega_{i,j}$ or $T_{i,j}$. Then

$$\begin{aligned} f^1_{i,j} &= \Big\{(I - A)\, f^o\Big\}_{i,j} \\ f^2_{i,j} &= \Big\{(I - B)\, f^1\Big\}_{i,j} \\ f^3_{i,j} &= \Big\{(I - C)\, f^2\Big\}_{i,j} \end{aligned} \tag{12}$$

which can be written

$$f^3_{i,j} = \Big\{(I - C)(I - B)(I - A) f^o\Big\}_{i,j} . \tag{13}$$

I is here the identity tensor, and A,B and C are tensors which calculate the changes produced in the three stages. The change produced by A is due to convection in the x-direction, that produced by B is due to convection in the y-direction, and that produced by C is due to the other terms of equation (9) and (11).

To calculate the change due to convection in the x-direction, a fourth-order curve is drawn through the points $f_{i-2,j}$, $f_{i-1,j}$, $f_{i,j}$, $f_{i+1,j}$, $f_{i+2,j}$ and the value of f on this curve corresponding to an x value of $(i \Delta x + u \Delta t)$ is calculated. Reduced to algebraic form this gives

$$\begin{aligned} (A f)_{i,j} = {} & \frac{\alpha}{12}\Big[8(f_{i+1,j} - f_{i-1,j}) - (f_{i+2,j} - f_{i-2,j})\Big] \\ & + \frac{\alpha^2}{24}\Big[30\, f_{i,j} - 16(f_{i+1,j} + f_{i-1,j}) + (f_{i+2,j} + f_{i-2,j})\Big] \\ & + \frac{\alpha^3}{12}\Big[-2(f_{i+1,j} - f_{i-1,j}) + (f_{i+2,j} - f_{i-2,j})\Big] \\ & - \frac{\alpha^4}{24}\Big[6\, f_{i,j} - 4(f_{i+1,j} + f_{i-1,j}) + (f_{i+2,j} + f_{i-2,j})\Big] \end{aligned} \tag{14}$$

where $\alpha = \dfrac{u_{i,j} \cdot \Delta t}{\Delta x}$.

Similarly

$$
\begin{aligned}
(Bf)_{i,j} = \frac{\beta}{12}\left[8(f_{i,j+1} - f_{i,j-1}) - (f_{i,j+2} - f_{i,j-2})\right] \\
+ \frac{\beta^2}{24}\left[30 f_{i,j} - 16(f_{i,j+1} + f_{i,j-1}) + (f_{i,j+2} + f_{i,j-2})\right] \\
+ \frac{\beta^3}{12}\left[-2(f_{i,j+1} - f_{i,j-1}) + (f_{i,j+2} - f_{i,j-2})\right] \\
- \frac{\beta^4}{24}\left[6 f_{i,j} - 4(f_{i,j+1} + f_{i,j-1}) + (f_{i,j+2} + f_{i,j-2})\right]
\end{aligned}
\tag{15}
$$

where $\beta = \dfrac{v_{i,j} \cdot \Delta t}{\Delta x}$ $\qquad (\Delta x = \Delta y)$.

The tensor C can be written

$$
(Cf)_{i,j} = \frac{\Delta t}{(\Delta x)^2} \cdot P \cdot \left[f_{i+1,j} + f_{i-1,j} + f_{i,j+1} + f_{i,j-1} - 4 f_{i,j}\right] + Q \quad . \tag{16}
$$

When f is ω in the above expression,

$$
P = 1 \ , \ Q = \frac{1}{2} \cdot \frac{Ra}{Pr} \frac{\Delta t}{\Delta x}\left(- T_{i+1,j} + T_{i-1,j}\right) \quad .
$$

When f is T in the above expression

$$
P = \frac{1}{Pr} \ , \ Q = \frac{\Delta t}{Pr}
$$

As has been noted by Crowley, even with

$$
|A| \ll 1, \quad |B| \ll 1, \quad |C| \ll 1
$$

the approximate form of equation (13)

$$f^{3}_{i,j} = \left\{(I - A - B - C)f^{o}\right\}_{i,j}$$

leads to serious error.

The case considered in Crowley's paper and the case considered here have two points in common.

(1) The spacial variation of the components of velocity (u,v) is slow.

(2) The spacial variation of the quantity being convected (ψ for Crowley's paper, T and ω for the present paper) is very rapid.

This fourth order method is most appropriate under these conditions.

4. Relaxation Method

To solve equation (10) (Poisson's equation), a relaxation method known as Liebmann's method was used. This method has been considered by Lance (5) and by Fromm (6). The method is now described.

A series of approximations $\psi^{1}_{i,j}$, $\psi^{2}_{i,j}$, --- $\psi^{n}_{i,j}$ - was obtained for the stream function at all mesh points. The approximation numbered (n + 1) was obtained from the approximation numbered n using the equation

$$\psi^{n+1}_{i,j} = \frac{1}{4}\left\{\psi^{n}_{i+1,j} + \psi^{n+1}_{i-1,j} + \psi^{n}_{i,j+1} + \psi^{n+1}_{i,j-1} + (\Delta x)^{2}\,\omega_{i,j}\right\} \quad . \quad (17)$$

Equation (17) was applied to all mesh points starting from i = 1, J = 1 and sweeping through the mesh with increasing i and J. As the sweep continued the n^{th} approximation was replaced by the $(n + 1)^{th}$. In the calculation the first approximation was taken as the solution from the previous time step. A series of approximations was calculated until a required degree of accuracy was obtained. This required degree of accuracy was defined by the condition

$$\mathrm{Max}\left(\left|\psi^{n+1}_{i,j} - \psi^{n}_{i,j}\right|\right) < R_{L} \cdot \mathrm{Max}\left(\left|\psi^{1}_{i,j}\right|\right) \quad . \quad (18)$$

The value of R_L was for most calculations 0.0002, thus equation (19) is similar to equation (3-2) of Fromm's report. The calculation was arranged so that condition (18) was tested once every n_s sweeps of the mesh points and the relaxation stopped when the condition was satisfied. For the most rapid

calculation it was found that n_s should have a value of about 3.

For all calculations there is the boundary condition that the component of velocity normal to the boundary is zero. The equation

$$\underline{u} = \text{curl } \underline{\psi}$$

gives

$$u = \frac{\partial \psi}{\partial y} \quad , \quad v = - \frac{\partial \psi}{\partial x} \tag{19}$$

The above boundary condition can be satisfied by making ψ zero at all boundary mesh points. Initially ψ was made zero at all boundary mesh points. The relaxation equation (17) was then applied to all the mesh points except those on the boundary, which remained zero throughout the calculation.

5. Boundary Conditions for Temperature (T), Vorticity (ω) and Stream Function (ψ)

The boundary conditions which may have to be satisfied are:

(1) Normal component of velocity zero,

(2) Tangential component of velocity zero,

(3) Temperature zero,

(4) Normal component of temperature gradient zero.

Condition (1) applies to all surfaces. Condition (2) applies to all surfaces where there is a solid in contact with the liquid, but does not apply to any free surfaces in the configuration. For any surface conditions (3) and (4) are mutually exclusive. Condition (3) applies to a heat conducting surface and condition (4) applies to a heat insulating surface. Condition (1) was satisfied by making $\psi = 0$ at all boundary points, and this has been explained in the previous section. Condition (3) was satisfied in a similar manner; T was initially made zero on the surfaces in question and remained zero throughout the calculation. To satisfy condition (4) the temperature at all mesh points except at the boundary was time advanced as described in section 3, then the temperature at the boundary mesh points was set to make the normal component of temperature gradient zero. The temperature at the mesh point adjacent to the boundary (i=2) and two away from the boundary (i=3) were considered.

These values of $T_{i,j}$ are plotted as points B and C in Fig 1. The boundary condition is now set by drawing a parabola through the points B and C to have zero slope at the boundary (i=1). This procedure leads to the equation

$$T_{1,j} = \frac{4}{3} T_{2,j} - \frac{1}{3} T_{3,j} \quad . \tag{20}$$

In the rest of this section the boundary condition (2) is discussed. This boundary condition is not only the most difficult to satisfy, but considerably complicates the task of running the complete program to a prescribed accuracy. From equation (19) condition (2) makes the gradient of the stream function normal to the boundary zero at the boundary. Thus from conditions (1) and (2), in the neighbourhood of the boundary $\psi = Cd^2$, where d is the distance from the boundary. Considering the boundary i = 1, this condition is satisfied by making

$$\psi_{2,j} = \frac{1}{4} \psi_{3,j} \quad . \tag{21}$$

This change is now made. However for equation (10) to be satisfied

$$\omega_{2,j} = \frac{1}{(\Delta x)^2} \left\{ 4 \psi_{2,j} - \psi_{1,j} - \psi_{3,j} - \psi_{2,j+1} - \psi_{2,j-1} \right\} \quad . \tag{22}$$

Thus $\omega_{2,j}$ must be given the value of equation (22). For all other surfaces where condition (2) is satisfied, ψ and ω at points adjacent to the boundary must be altered to satisfy equations similar to (21) and (22). The relaxation process described in section 4 must be repeated with the new values of ω at points adjacent to the boundary. This further relaxation usually took fewer sweeps. ω must now be specified at points on the boundary. Following Fromm the normal component of the gradient of ω was made zero at the boundary. The values of ω on the boundary were then given by equations similar to equation (20):

$$\omega_{1,j} = \frac{4}{3}\omega_{2,j} - \frac{1}{3}\omega_{3,j} \quad . \qquad (23)$$

This boundary condition can not be deduced. However it can be shown from the basic equations that the average value of the normal gradient of ω at the boundary is zero. These values of ω at the boundary have only a small effect on the rest of the calculation.

6. Initial Conditions

For the initial conditions the temperature T, the vorticity ω and the stream function ψ must be specified at all mesh points, and the boundary conditions given in section 5 must be satisfied. Further equation (10) relating ψ and ω must be satisfied.

For all the cases so far computed, ω has been specified and ψ calculated to satisfy equation (10) using the relaxation method of section 4. The values of ω at the mesh points have been generated by a random number program so that values of -S, 0 and +S occurred with equal probability. To satisfy the boundary conditions it was necessary to use an iterative method. The following three steps were repeated in sequence:

(1) solve equation (10) by the relaxation method,

(2) use an equation similar to equation (21)

to recalculate ψ at all mesh points adjacent to the boundary,

(3) use an equation similar to equation (22) to recalculate ω at all mesh points adjacent to the boundary.

The sequence of these three steps must be repeated 10 or 20 times for the values of ω and ψ adjacent to the boundary to converge. Finally ω at mesh points on the boundary must be calculated using equations similar to equation (23).

For the initial values of the temperature T the first computer calculation took the steady state conduction solution. Taking $\frac{\partial T}{\partial t} = 0$ and $\underline{u} = 0$ in equation (5) gives

$$\Delta^2 T = -1 \qquad (24)$$

The solution of equation (24), with the correct boundary conditions, can be obtained by a relaxation method, but for the cases considered it was a simple parabolic function. It was found that this gave an initial value of mean temperature $\overline{T}$ which was too large, and the computing time to reach the value of $\overline{T}$ for thermal equilibrium was very large. For subsequent computer calculations the initial temperature distribution was scaled down by a factor f_T to give an initial mean temperature $\overline{T}$ which was approximately correct.

7. A Method for Improving the Accuracy of the Calculation

The accuracy of the method of calculation described in section 3 to section 6 was estimated by a method now to be described. A solution for temperature, vorticity and stream function obtained from a previous calculation was taken. Write this solution $T_{i,j} = T^0_{i,j}$, $\omega_{i,j} = \omega^0_{i,j}$. The calculation was then time advanced by a single time-step length Δt and the solution $T_{i,j} = T^1_{i,j}$ $\omega_{i,j} = \omega^1_{i,j}$ was saved. The process was then repeated starting with the solution $T_{i,j} = T^0_{i,j}$, $\omega_{i,j} = \omega^0_{i,j}$ but now time advancing the solution by four time steps of length $\frac{\Delta t}{4}$ to give a solution $T_{i,j} = T^2_{i,j}$, $\omega_{i,j} = \omega^2_{i,j}$. The change produced at each mesh point for the calculated quantities

$$\Delta T_{i,j} = T^2_{i,j} - T^0_{i,j} \ , \ \Delta \omega_{i,j} = \omega^2_{i,j} - \omega^0_{i,j}$$

was calculated and printed out. Also the error produced at each mesh point for the calculated quantities

$$\epsilon T_{i,j} = T^2_{i,j} - T^1_{i,j} \ , \ \epsilon \omega_{i,j} = \omega^2_{i,j} - \omega^1_{i,j}$$

was calculated and printed out. Then meaning over the cross section write

$$\Delta T_s = \sqrt{\left\{ \overline{(\Delta T_{i,j})^2} \right\}} \ , \ \Delta \omega_s = \sqrt{\left\{ \overline{(\Delta \omega_{i,j})^2} \right\}} \ .$$

Then a measure of the relative error at each mesh point is given by the equations

$$\left(W_T\right)_{i,j} = \frac{T^2_{i,j} - T^1_{i,j}}{\Delta T_s} \ , \ \left(W_\omega\right)_{i,j} = \frac{\omega^2_{i,j} - \omega^1_{i,j}}{\Delta \omega_s} \ .$$

Here high accuracy leads to small values of $(W_T)_{i,j}$, $(W_\omega)_{i,j}$. It was found that for all mesh points $(W_T)_{i,j}$ was of the order of 0.01. If mesh points on

the boundary, adjacent to the boundary and two away from the boundary were excluded $(W_\omega)_{i,j}$ was also of the order of 0.01. For points on or adjacent to the boundary $(W_\omega)_{i,j}$ was as much as 0.5 and for points two away from the boundary it was as much as 0.1. The quantity R_L of equation (19), which controls the accuracy to which the relaxation solution of equation (10) is carried out, was given a value 0.0002. Larger values of R_L made the values $(W_\omega)_{i,j}$ greater and hence the accuracy poorer. Smaller values of R_L did not much change the values of $(W_\omega)_{i,j}$.

The method for the improvement of the accuracy, to be described, attempts to improve the accuracy at points two away from the boundary, which will be called the C-points. For these points the velocity of the liquid was small and thus the convection term of equation (9) was small, but the diffusion term was often larger than average. Thus it can no longer be assumed that the convective term is larger than the diffusive term. For the diffusive term

$$(\omega)_{t+\Delta t} = (\omega)_t + \left(\frac{\partial \omega}{\partial t}\right)_t . \Delta t \quad .$$

However a much better approximation is given by

$$(\omega)_{t+\Delta t} = (\omega)_t + \left(\frac{\partial \omega}{\partial t}\right)_{t+\frac{\Delta t}{2}} . \Delta t \quad . \qquad (25)$$

For the C-points the calculation of the change produced by the diffusive term was made using equation (25). The calculation for a single time step is now as follows:

(1) Time advance the vorticity ω for all mesh points as described in section 3.

(2) Save the change produced in the last stage of equation (12), that is:

$$\Delta \omega_c = f^3_{i,j} - f^2_{i,j}$$

for the C-points only. This change is stored in a special array.

(3) Calculate the average of the initial and final values of ω at each

mesh point and store in a special array

$$\left(\omega_{av}\right)_{i,j} = \frac{1}{2}\left(\omega_t + \omega_{t+\Delta t}\right)_{i,j} .$$

(4) Solve equation (10) for Ψ with $\omega = \omega_{av}$ using the relaxation method of section 4.

(5) Recalculate ω and Ψ at points adjacent to the boundary to suit boundary conditions using equations (21) and (22) and similar equations.

(6) Solve equation (10) for Ψ by the relaxation method with the new values of ω adjacent to the boundary.

(7) For the C-points subtract the $\Delta\omega_c$ previously calculated and add a recalculated value of $\Delta\omega_c$ obtained using equation (16) and the ω of stage (5) above.

(8) Calculate new values of ω for points adjacent to the boundary assuming a linear rate of change of ω with time using the equation

$$\left(\omega_{t+\Delta t}\right)_{i,j} = \left(\omega_{av}\right)_{i,j} + \left(\omega_{av} - \omega_t\right)_{i,j} .$$

(9) Solve equation (10) for Ψ by the relaxation method with $\omega = \omega_{t+\Delta t}$ as calculated in stages (1), (7) and (8).

(10) Recalculate ω and Ψ at points adjacent to the boundary using equations (21) and (22) and similar equations.

(11) Solve equation (10) for Ψ by the relaxation method with the new values of ω adjacent to the boundary.

(12) Time advance the temperature T for all mesh points except points on the boundary as described in section 3.

(13) For mesh points on the boundary of heat-insulating surfaces use equation (20) and similar equations to calculate the temperature T.

When the proceedure of stages (1) to (13) above was used, $(W_\omega)_{i,j}$ at points on the boundary and adjacent to the boundary was at the most 0.05, a decrease by a factor of 10. $(W_\omega)_{i,j}$ for the C-points was at the most 0.01. When this improvement in accuracy was noted, the method was used for all subsequent calculation. It has been used in all the numerical results given in this report.

8. Estimation of Accuracy and Adjustment of Time-step Length

$\omega^{o}_{i,j}$, $\omega^{1}_{i,j}$, $\omega^{2}_{i,j}$ and ΔW_S are as defined in section 7, and

$$\epsilon\,\omega_s = \sqrt{\left\{\overline{(\epsilon\,\omega_{i,j})^2}\right\}} \quad .$$

It is required to run a program so that $X = \epsilon\,\omega_S/\Delta\omega_S$ is less than some predetermined value. Over a certain range of time-step length Δt, X varied approximately linearly with Δt. However there was a minimum value of X which could be obtained and further reduction of Δt did not reduce X, which was found to vary in an irregular manner under these conditions. This minimum value of X varied with time as the program was run. This made it difficult to run a program with automatic adjustment of the time-step length. It was found convenient to define a corrected value of X by the equation

$$X_c = \frac{\epsilon\,\omega_s}{\Delta\,\omega_s + f_q.\max(|\omega|)} \quad .$$

The error $\epsilon\omega_S$ and hence X_c can be decreased indefinitely by decreasing the time-step length Δt. Two numbers A_{max} and A_{min} were set and the program was arranged so that when $X_c > A_{max}$ the time-step length Δt was halved, and when $X_c < A_{min}$ the time-step length Δt was doubled. In order to prevent frequent changes in time-step length $A_{max}/A_{min} = 2.5$.

Jahn and Reineke considered the stability of the numerical procedure and calculated a maximum time-step length for stability. The program was then run with the time-step length a certain fraction of the critical time-step length. This makes the time-step length greater by at least a factor of two than the time-step length for cases with the present program.

9. Organisation of the Program

Appendix 1 gives a key to all the symbols used in the computer program, and Appendix 2 gives a list of all the subroutines used with an explanation of their purpose. Appendix 3 gives a listing of a shortened version of the MAIN computer program and Appendix 4 gives a listing of the subroutine FSTEP

which calculates stages (1) to (13) of section 7.

In the MAIN program, at the beginning the quantities $T_{i,j}$, $\omega_{i,j}$, $\psi_{i,j}$, t and various constants of the problem were read in from a data set 2, which is a disc file. The program was then run for NMAX cycles. In each cycle NSTEP time steps were taken, and at the end of the cycle the solution obtained ($T_{i,j}$, $\omega_{i,j}$, $\psi_{i,j}$, t) was written to a data set 3, which for long runs was a tape. At the end of the program the quantities $T_{i,j}$, $\omega_{i,j}$, $\psi_{i,j}$, t and various constants of the problem were written to a data set 4, which was a disc file. This disc file was used as the data set 2 for the input to the next run of the program. Graphical output or further calculation on the solution must be obtained by running a separate program reading from the tape.

The automatic adjustment of time-step length takes place after the first time step in a cycle has been made. The method is as described in section 8. The number of sweeps in the relaxing subroutine varied in an unpredictable manner, and consequently the computing time was unpredictable. In order to insure that there was a file to start the next run the following procedure was adopted. The central processor time was called at the end of each cycle and if this exceeded a time TIMAX the program ended with the solution being written to data set 4. The time TIMAX was sufficiently less than the time limit for the program to prevent this time being reached. In order to estimate the accuracy in the main program it was necessary to duplicate the arrays for $T_{i,j}$, $\omega_{i,j}$ and $\psi_{i,j}$. Further in the subroutine FSTEP in order to calculate from equation (12) it was necessary to introduce two extra arrays AT1(I,J) and AT2(I,J). These extra arrays increased the sizes of the program. The space required to run a program with arrays of 81 x 41 mesh points is 220 K bytes.

10. Comparison of Calculated Results with the Experimental Results of Ralph and Roberts

In the experiments of Ralph and Roberts there was uniform generation of heat

per unit volume in a liquid contained in a tank of rectangular cross-section. The top surface of the tank was cooled to a constant temperature, but the other surfaces were heat insulating. Measurements were made of the temperature within the liquid under conditions of thermal equilibrium. The measurements were made for a range of Rayleigh number from 10^5 to 10^9 for very dilute hydrochloric acid at 30^0C which corresponds to a Prandtl number of 5.39. For the calculation the tank cross section was taken to have a width to depth ratio of two; that is a depth of one normalised unit and a width of two normalised units. The calculation was made for Rayleigh numbers of $5.0\text{x}10^5$, $5.0\text{x}10^6$ and $5.0\text{x}10^7$ and for a Prandtl number of 5.39. Initially the mesh size was 51 x 26 which was adequate for Rayleigh numbers of $5.0\text{x}10^5$ and $5.0\text{x}10^6$ but not for $5.0\text{x}10^7$. For the case with a Rayleigh number of $5.0\text{x}10^7$ the mesh size was changed to 81 x 41 later in the calculation.

The initial conditions were set as described in section 6 with S = 100.0. Fig 2 shows the time variation of $\sqrt{(u^2+v^2)}$ the root mean square velocity in normalised units,meaned over the channel cross section. The peak at the beginning of this curve corresponds to the movement of hot liquid, initially at the bottom of the channel, towards the top of the channel. Fig 3 shows isothermals for the liquid temperature and stream lines for the liquid flow at this time. Fig 4 shows the time variation of the mean temperature of the liquid $\overline{T}$. The initial part of this curve, where there is a high rate of rise of temperature, corresponds to the condition where the rate of generation of heat within the liquid was not balanced by a flow of heat tothe top surface. The curve peaks and there is then for a time a fall in mean temperature. This corresponds to the establishment of a high temperature gradient in the liquid near the top surface and hence a large flow of heat out of the liquid. This large temperature gradient is produced by the initial surge of liquid. This is followed by a slowly rising temperature with superimposed oscillations as conditions for thermal equilibrium are approached. The curves of figs 2 and 4 are for a Rayleigh number of $5.0\text{x}10^6$, but similar curves were obtained for the other Rayleigh

numbers.

If the curve of fig 4 was continued long enough thermal equilibrium would be reached where the instantaneous mean temperature $\bar{T}$ oscillated about a time - averaged mean temperature $\bar{\bar{T}}$. The oscillation in mean temperature was produced by a continual change of the flow pattern within the liquid. That is the motion of the liquid was turbulent. This calculated turbulent flow condition corresponds to the turbulent flow inferred from temperature measurements in the experiment. The frequency and amplitude of the temperature oscillations at a point on the cross section obtained from the calculation correspond to the measured values. The calculation run times have so far been too short for quantitative comparison. Fig 5 shows isothermals within the liquid for a series of different times. For the last of these times contour plots for the vorticity and stream function are included. This clearly illustrates that the vorticity is obtained approximately by integrating the horizontal gradient of the temperature over time. The intermittent jet of cool liquid flowing down from the top surface of fig 5 resembles the photographs of Jahn and Reineke (7) who used a holographic technique.

Write T_L' and T_C' for the temperature in degrees Celsius. T_L' is the average temperature at the heat-insulating bottom surface and T_C' is the temperature of the top surface. Then equation (10) of the report by Ralph and Roberts is

$$M_L = \frac{H L^2}{2k(T_L' - T_c')} \quad .$$

In the normalised units of this report

$$T_L = (T_L' - T_c') / \frac{HL^2}{k}$$

$$\therefore \quad M_L = \frac{1}{2\ T_L} \quad .$$

Fig 6 shows three values of M_L obtained from this calculation plotted on a graph of M_L against Ra. The experimental points from the report of Ralph and Roberts are included for comparison.

The method of section 8 where the time-step length was adjusted to obtain a required accuracy was used for the earlier part of the calculation. It was possible to run the program with a value of about 0.1 for X. As the condition for thermal equilibrium was approached this program was changed, and a program was used where the time-step length was constant. The value of Δ_ω was then small and varied as the flow pattern changed, whereas the value of $\epsilon\omega$ was more nearly constant. The range of variation of X for different Rayleigh numbers is shown in table 1. For the case with a Rayleigh number of 5.0×10^5 X is large. A possible reason for this is that the number of sweeps taken per call of the relaxation routine is now approximately two. When the method of section 7 was used to estimate the accuracy on reducing Δt to $\Delta t/4$ a single sweep of the relaxation routine per call would keep the accuracy better than the limit set by equation (18).

For the case with a Rayleigh number of 5.0×10^7 the mesh size of 51 x 26 was too coarse. This became apparent when contour plots of the liquid temperature were examined. Large temperature gradients were produced and the change in temperature in a single mesh space became an appreciable fraction of the maximum temperature. Under these conditions the solution for the temperature shows oscillations in space on either side of this large change. Fig 7 shows contour plots of the temperature for the same conditions using (a) a mesh of 51 x 26 and (b) a mesh of 81 x 41.

The improvement on changing to the finer mesh is apparent. However if the time-step length Δt remains unchanged the accuracy defined by X remains almost unchanged.

From an examination of contour plots, it was apparent that the value of two for the ratio of channel width to channel height was too small. The jets of cooled liquid from the top surface were frequently close to the end boundary walls, which effected the flow pattern. In their latest results Jahn and Reineke (7)

have used a width to height ratio of about four.

11. Comparison of Calculated Results with the Experimental Results of Wilkie and Fisher

The experiment of Wilkie and Fisher was also made with a liquid in which there was a uniform generation of heat; the liquid in this case was 20% aqueous zinc chloride. The liquid was enclosed in a rectangular region bounded by two vertical cooled walls, whose height and width were greater than their separation. The other boundary surfaces were heat insulating. The actual size of the apparatus was 100 cm (high) x 10 cm x 4 cm. The temperature variations within the liquid was measured using a Mach-Zehnder interferometer, and by a thermocouple. The liquid velocity was also measured by timing the motion of 'Perspex' particles. If the liquid was assumed to have the same physical properties as water, the range of values for the Rayleigh number would be 5.0×10^7 - 5.0×10^8. The motion of the liquid was nearly laminar but some small eddies were observed.

The calculation was unfortunately made before the paper by Wilkie and Fisher had been read. A tank with a height to width ratio of five was taken; that is a height of five normalised units and a width of one normalised unit. The mesh size taken was 21 x 101, the Rayleigh number was 5.0×10^6 and the Prandtl number was 5.39. The initial conditions were set as described in section 6 with S = 10.0. With no previous experience f_T was given a value of 0.1; this gave an initial value for the mean temperature too small by at least a factor of four. Fig 8 shows the time variation of the root mean square velocity $\sqrt{(u^2 + v^2)}$ in normalised units, and fig 9 shows the time variation of the mean temperature $\overline{T}$. Fig 10 shows contour plots for the temperature, vorticity and stream function for the time at which the calculation was stopped. From the contour plots of fig 10 the variation of temperature

and velocity across the middle of the channel may be obtained which closely resemble the experimental curves of fig 6 and fig 7 in the paper by Wilkie and Fisher.

The calculation, if continued, would clearly produce a time - invariant solution at thermal equilibrium. So running the calculation with a pre-determined value of X is not important. At the start of the calculation the time-step length was adjusted to run the program with $X < 0.1$. This however had to be abandoned and the program run with a constant value of the time-step length Δt. The value of Δw soon became small and X of the order of unity.

An examination of fig 10 shows that the vorticity at the vertical boundary is greater than the vorticity elsewhere by a factor of 2.5. Further the vorticity rises to this value from zero in approximately two mesh spaces. A consideration of the method of calculation used, suggests that the approach to the final laminar solution should be made with the mesh spacing at least halved. That is with a mesh of 41 x 201.

12. Further Checks on the Accuracy of Calculation

Bars over a symbol are used to denote the average value over the cross section. The integral $\int dV$ denotes integration over the volume in unit length of the channel and $\int dS$ denotes integration over the surface enclosing unit length of the channel.

Gauss's theorem gives

$$\int \nabla^2 \psi \, dV = \int \frac{\partial \psi}{\partial n} \, dS \quad .$$

But from the boundary conditions of section 5

$$\frac{\partial \psi}{\partial n} = 0 \quad ,$$

$$\therefore \int \nabla^2 \psi \, dV = 0 \quad ,$$

and from equation (10)

$$\int \omega \, dV = 0 \quad ,$$

that is $\overline{w} = 0$. (26)

Green's theorem for the stream function ψ may be written

$$\int \psi \frac{\partial \psi}{\partial n} \, dS = - \int \left\{ \left(\frac{\partial \psi}{\partial x} \right)^2 + \left(\frac{\partial \psi}{\partial y} \right)^2 \right\} dV - \int \psi \nabla^2 \psi \, dV \quad . \qquad (27)$$

From the boundary conditions of section 5

$$\int \psi \frac{\partial \psi}{\partial n} \, dS = 0 \quad .$$

From equation (10)

$$- \int \psi \nabla^2 \psi \, dV = \int \psi \omega \, dV \quad .$$

Then, using equation (19), equation (27) becomes

$$\int (u^2 + v^2) \, dV = \int \psi \omega \, dV \quad ,$$

that is

$$\overline{u^2 + v^2} = \overline{\psi\omega} \quad . \tag{28}$$

Under the conditions of the calculation, it was found that

$$\frac{\bar{\omega}}{\sqrt{\left(\overline{\omega^2}\right)}} = C_1 \approx 0.001$$

and

$$\frac{\overline{u^2+v^2} - \overline{\psi\,\omega}}{\overline{u^2+v^2}} = C_2 \approx 0.01 \quad .$$

The value of C_2 depends on the value of R_L taken in equation (18) which defines the accuracy to which the relaxation calculation is taken. For $R_L > 0.0002$, $C_2 > 0.01$, but for $R_L < 0.0002$, $C_2 \approx 0.01$. The above value of C_2 is for a mesh of 51 x 26 points. On changing to a mesh of 81 x 41 points the value of C_2 decreased to 0.005.

Integrating both sides of equation (5)

$$\int \frac{dT}{dt}\, dV = \frac{1}{Pr} \int (\nabla^2 T + 1)\, dV \quad .$$

Using Gauss's theorem, and writing the cross-sectional area of the channel A_c

$$\frac{d\bar{T}}{dt} = \frac{1}{Pr\ A_c} \int \frac{\partial T}{\partial n}\, dS + \frac{1}{Pr} \quad . \tag{29}$$

Considering a conducting surface i = 1,

then to a first approximation

$$\left(\frac{\partial T}{\partial n}\right)_1 = \frac{T_{2,j}}{\Delta x} \quad .$$

and to a second approximation

$$\left(\frac{\partial T}{\partial n}\right)_2 = \frac{2.T_{2,j} - \frac{1}{2} . T_{3,j}}{\Delta x}$$

When the above approximations are substituted into equation (29) two approximations are obtained for $\frac{d\bar{T}}{dt}$, say $\left(\frac{d\bar{T}}{dt}\right)_1$ and $\left(\frac{d\bar{T}}{dt}\right)_2$.

Let two values of $\bar{T}$, $\bar{T}_a$ and $\bar{T}_b$ be calculated at two not very different times t_a and t_b. Then a third approximation for $\frac{d\bar{T}}{dt}$ can be obtained from

$$\left(\frac{d\bar{T}}{dt}\right)_3 = \frac{\bar{T}_b - \bar{T}_a}{t_b - t_a} \quad .$$

After the initial transient $\left(\frac{dT}{dt}\right)_3$ was found to lie between the values $\left(\frac{d\bar{T}}{dt}\right)_1$ and $\left(\frac{d\bar{T}}{dt}\right)_2$. Agreement was better at low Rayleigh number.

13. Conclusion

From the calculation made so far there is no significant discrepancy between calculation and the results of previous experiments. This shows that, for the configurations considered, the assumption of two-dimensional flow is a good one.

The calculation has the disadvantage that it requires long computing times. For the cases considered in section 10 the time was 40 minutes on the Harwell computer (IBM System/360, model 75). This time would increase with the number of mesh points used, varying roughly linearly. So calculations at higher Rayleigh numbers where a finer mesh is required would require more computer time.

A number of changes in the program have been considered which might give a shorter computing time, but it does not appear possible to shorten the computing time by more than 30%.

Table 1

Rayleigh Number Ra =	X $\epsilon\omega_S/\Delta\omega_S$	Time-step Length Δt (Normalised Units)
$5.0.10^5$	0.3 – 0.5	$8.0.10^{-5}$
$5.0.10^6$	0.05 – 0.3	$4.0.10^{-5}$
$5.0.10^7$	0.05 – 0.1	$2.0.10^{-5}$

References

[1] RALPH, J. C. and ROBERTS, D. N. Free Convection Heat Transfer Measurements in Horizontal Liquid Layers with Internal Heat Generation. AERE-R7841 (1974).

[2] WILKIE, D. and FISHER, S. A. Natural Convection in a Liquid Containing a Distributed Heat Source. Int. Develop. in Heat Transfer 5, (1961) 995.

[3] JAHN, M. and REINEKE, H. H. Free Convection Heat Transfer with Internal Heat Sources Calculations and Measurements. 5th International Heat Transfer Conference, Tokyo, September 3-7 1974. Paper NC2.8

[4] CROWLEY, W. P. Numerical Advection Experiments. Monthly Weather Review, 96, (1968) 1.

[5] LANCE, G. N. Numerical Methods for High-Speed Computers. Iliffe and Sons Ltd. London (1960).

[6] FROMM, J. E. A Method for Computing Nonsteady, Incompressible, Viscous Fluid Flows. Los Alamos Scientific Laboratory, New Mexico. LA-2910 (1963).

[7] JAHN, M. and REINEKE, H. H. Privately Communicated (1974).

Computer Symbols used in MAIN program and in Subroutine FSTEP

Computer Symbol	Mathematical Symbol	
TEMP(I,J), TEMPA(I,J)	$T_{i,J}$	
OMEGA(I,J), OMEGAA(I,J)	$\omega_{i,J}$	
PSI(I,J),PSIA(I,J)	$\psi_{i,J}$	
AT1(I,J),AT2(I,J)	$T_{i,J}$ or $\omega_{i,J}$	Temporary arrays used in the solution of equation (12)
G(I)	ΔW_C	Array used for the C-points
AMAG	S	
CRAT	X_C	
DELT	Δt	
DELTLM		Smallest value of Δt allowed
DELX	Δx	
ERRAT/2.0	A_{max}	
ERRAT/5.0	A_{min}	
FQ	f_q	
FT	f_T	
IP		A switch used to print out the number of sweeps in the relaxation routine
IR		Parameter used to control the random number routine used to determine initial values of ω.
IRUN		Run number
NMAX		Number of cycles in run
NS	n_s	
NSTEP		Number of time steps in cycle
NSR		Series number
NX		Mesh Size
NY		
ORAT	X	

Computer Symbol	Mathematical Symbol
PR	Pr
RA	Ra
RELRAT	R_L
T	t

Computer Subroutines used in MAIN program and in Subroutine FSTEP

SUBROUTINE RRLAX (PSI, OMEGA, PLIM, NS, MM)

Calculates stages (4), (5) and (6) or stages (9), (10) and (11) of the proceedure in section 7. PSI, OMEGA and NS are as in the MAIN routine. PLIM is equal to the right hand side of equation (18) and controls the relaxation solution. MM(2) is an array which returns the number of sweeps in the first and second call of the relaxation subroutine.

SUBROUTINE ACAL1 (A1, A2, P, RAT, IW)

Solves the first part of equation (12)

$$f^{1}_{i,i} = \{(I-A)f^{o}\}_{i,j}$$

with A2(I,J) for $f^{1}_{i,j}$ and A1(I,J) for $f^{o}_{i,j}$. P is the stream function ψ from which the velocity u is obtained using equation (19). RAT = $\frac{\Delta t}{2(\Delta x)^2}$

IW is a switch set to -1 when the stability condition for the calculation is violated.

SUBROUTINE ACAL2 (A1, A2, P, RAT, IW)

Solves the second part of equation (12)

$$f^{2}_{i,j} = \{(I-B)f^{1}\}_{i,j}$$

with A2 (I,J) for $f^{2}_{i,j}$ and A1(I,J) for $f^{1}_{i,j}$. P is the stream function from which the velocity v is obtained using equation (19). RAT = $\frac{\Delta t}{2(\Delta x)^2}$

IW is a switch set to -1 when the stability condition for the calculation is violated.

SUBROUTINE ACAL3 (A1, A2, T, G, CPR, DELT)

Calculates stage (7) of the proceedure in section 7. A1 is the ω obtained in stage (5) and A2 is the ω to be used in stage (9). T is the temperature array

$T_{i,j}$ and G is an array used to store $\Delta\omega_C$ for the C-points. CPR and DELT are as in the MAIN program.

SUBROUTINE ACALG(A1, A2, G)

Calculates stage (2) of the proceedure in section 7. That is

$$\Delta W_C = f^3_{i,j} - f^2_{i,j}$$

with A2(I,J) for $f^3_{i,j}$ and A1(I,J) for $f^2_{i,j}$. The changes ΔW_C for the C-points are stored in the array G.

SUBROUTINE ACALT (A1, A2, RPR, DELT)

Solves the third part of equation (12)

$$f^3_{i,j} = \{(I-C)f^2\}_{i,j}$$

with A2(I,J) for $f^3_{i,j}$ and A1(I,J) for $f^2_{i,j}$ and $f_{i,j}$ now representing the temperature array $T_{i,j}$. RPR and DELT are as for the MAIN program.

SUBROUTINE ACALW(A1, A2, T, CPR, DELT)

Solves the third part of equation (12)

$$f^3_{i,j} = \{(I-C)f^2\}_{i,j}$$

with A2(I,J) for $f^3_{i,j}$ and A1(I,J) for $f^2_{i,j}$ and $f_{i,j}$ now representing the vorticity array $\omega_{i,j}$. T is the temperature array $T_{i,j}$ and CPR and DELT are as for the MAIN program.

SUBROUTINE ARMAX (AR, AMAX, AMIN, IS)

With IS = 1 this subroutine selects the maxiumum absolute value AMAX of an array. AR(I,J).

SUBROUTINE DIFRMS (A1, A2, DIF)

Calculates the root mean square value DIF of the difference between the two arrays A1(I,J) and A2(I,J)

SUBROUTINE ADIF(AR, BR, CR)

Sets the array CR(I,J) equal to the array AR(I,J) minus the array (BR(I,J).

SUBROUTINE AEQ(AR,BR)

Sets the array BR(I,J) equal to the array AR(I,J)

Listing of MAIN Program

```
      DIMENSION TEMP(51,26), OMEGA (51,26), PSI(51,26), TEMPA(51,26),
     (Cond) OMEGAA(51,26), PSIA(51,26)
      COMMON NX,NY,DELX
      NAMELIST/INPUT1/NSR,IRUN,ERRAT,RELRAT,DELTLM, TIMAX
     (Cond) NSTEP,NMAX,NS,IP,FQ
      NREAD = 5
      READ(NREAD,INPUT1)
      READ(2)((TEMP(I,J),J = 1,26), I= 1,51), ((OMEGA(I,J),J = 1,26),I = 51),
     (Cond) ((PSI(I,J), J= 1,26),I = 1,51),RA,PR,AMAG,IR,FT,DELT,T,DELX,NX,NY
      CPR = RA/PR
      RPR = 1.0/PR
      IYY = NMAX
      CX = 0.25 *DELX*DELX
    8 IV = 1
   10 CALL AEQ(TEMP,TEMPA)
      CALL AEQ(OMEGA,OMEGAA)
      CALL AEQ(PSI,PSIA)
      DT = 0.25*DELT
      IY = 4
   11 CALL FSTEP(TEMPA,OMEGAA,PSIA,DT,CPR,RPR,RELRAT,0,IP)
      IY = IY-1
      IF(IY)12,12,11
   12 CALL ARMAX(OMEGA,OMAX,OMIN,1)
      CALL DIFRMS(TEMP,TEMPA,TDIF)
      CALL DIFRMS(OMEGA,OMEGAA,ODIF)
      CALL DIFRMS(PSI,PSIA,PDIF)
```

```
      CALL FSTEP(TEMP,OMEGA,PSI,DELT,CPR,RPR,RELRAT,0,IP)
      T = T + DELT
      CALL DIFRMS(TEMP,TEMPA,TERR)
      CALL DIFRMS(OMEGA,OMEGAA,OERR)
      CALL DIFRMS(PSI,PSIA,PERR)
      PRINT 13, TDIF,ODIF,PDIF,TERR,OERR,PERR
13    FORMAT (-)
      CRAT = OERR/(ODIF+FQ*OMAX)
      IF(ERRAT-2.0*CRAT)15,14,14
14    IF(5.0*CRAT-ERRAT)16,20,20
15    DELT = 0.5*DELT
      IV = -1
      IF (DELT-DELTLM)29,29,10
16    IF(IV)20,17,17
17    DELT = 2.0 * DELT
      IF(DELT-CX)10,18,18
18    DELT = 0.5*DELT
20    IY = NSTEP
22    CALL FSTEP(TEMP,OMEGA,PSI,DELT,CPR,RPR,RELRAT,NS,IP)
      T = T + DELT
      IY = IY - 1
      IF(IY)26,26,22
26    TIME = ZA02AS(DUMMY)
      WRITE(3)((TEMP(I,J), J=1,26),I=1,51),((OMEGA(I,J),J=1,26),I=1,51),
      (Cond) ((PSI(I,J), J=1,26),I=1,51),T
      IF(TIMAX-TIME)28,28,27
27    IYY = IYY-1
      IF(IYY)28,28,8
28    WRITE(4)((TEMP(I,J),J=1,26),I=1,51),((OMEGA(I,J),J=1,26),I=51),
      (Cond)((PSI(I,J),J=1,26),I=1,51),RA,PR,AMAG,IR,FT,DELT,T,DELX,NX,NY
29    STOP
      END
```

Listing of Subroutine FSTEP

```
      SUBROUTINE FSTEP(TEMP,OMEGA,PSI,DELT,CPR,RPR,RELRAT,NS,IP)
      DIMENSION PSI(51,26),TEMP(51,26),OMEGA(51,26),AT1(51,26),
     (COND)AT2(51,26),G(134),MA(2),MB(2)
      COMMON NX,NY,DELX
      NXA = NX-1
      NYA = NY-1
      NYB = NY-2
      CONDEL = 0.5/DELX/DELX
      CALL ARMAX(PSI,PMAX,PMIN,1)
      PLIM = RELRAT*PMAX
      RAT = CONDEL*DELT
      CALL ACAL1(OMEGA,AT1,PSI,RAT,IW)
      CALL ACAL2(AT1,AT2,PSI,RAT,IW)
      CALL ACALW(AT2,ATI,TEMP,CPR,DELT)
      CALL ACALG(AT2,AT1,G)
      CALL ADIF(AT1,OMEGA,AT2)
      DO 5 I = 2, NXA
      DO 4 J = 2,NYA
    4 AT2(I,J) = OMEGA(I,J) +0.5*AT2(I,J)
    5 CONTINUE
      CALL RRLAX(PSI,AT2,PLIM,NS,MA)
      CALL ACAL3(AT2,AT1,TEMP,G,CPR,DELT)
      DO 6 I = 2,NXA
      AT1(I,2)=2.0*AT2(I,2)-OMEGA(I,2)
    6 AT1(I,NYA)=2.0*AT2(I,NYA)-OMEGA(I,NYA)
```

```
      DO 7 J = 3,NYB
      AT1(2,J) = 2.0*AT2(2,J)-OMEGA(2,J)
    7 AT1(NXA,J)=2.0*AT2(NXA,J)-OMEGA(NXA,J)
      CALL RRLAX(PSI,AT1,PLIM,NS,MB)
      CALL AEQ(AT1,OMEGA)
      CALL ACAL1(TEMP,AT1,PSI,RAT,IW)
      CALL ACAL2(AT1,AT2,PSI,RAT,IW)
      CALL ACALT(AT2,TEMP,RPR,DELT)
      IF(IP)17,17,15
   15 PRINT 16,MA(1),MA(2),MB(1),MB(2)
   16 FORMAT(10 X, 12H FROM,FSTEP, 4I4)
   17 RETURN
      END
```

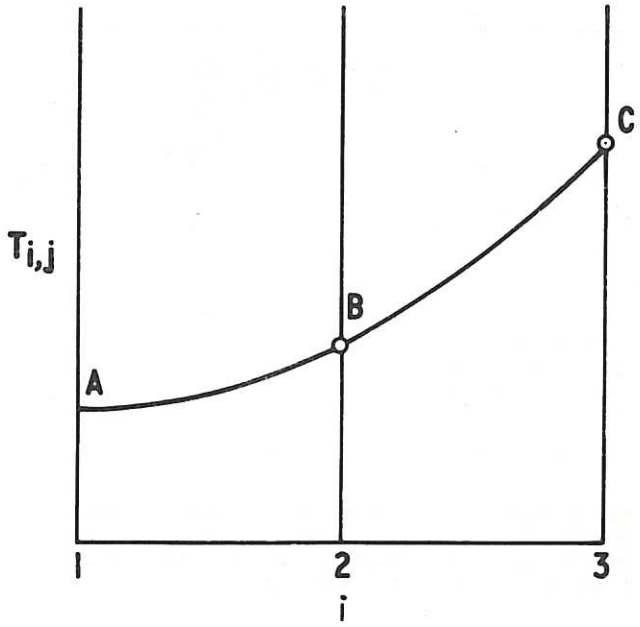

Fig.1 Boundary condition with zero gradient normal to the boundary.

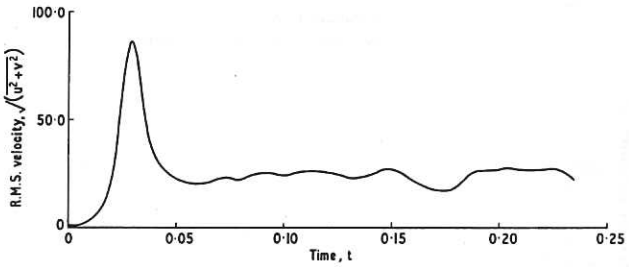

Fig.2 Calculated time variation of the root mean square velocity for the case of Ralph and Roberts. Ra = $5.0.10^6$, Pr = 5.39, width to height ratio = 2.

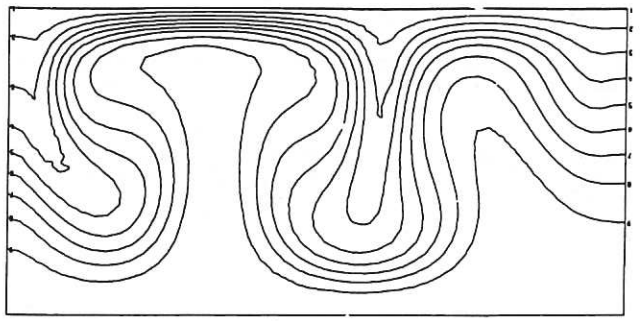

(a) Isothermals.
Temperature contour heights: 1 = 0.0, 2 = 0.02, 3 = 0.04, 4 = 0.06, 5 = 0.08, 6 = 0.10, 7 = 0.12, 8 = 0.14, 9 = 0.16.

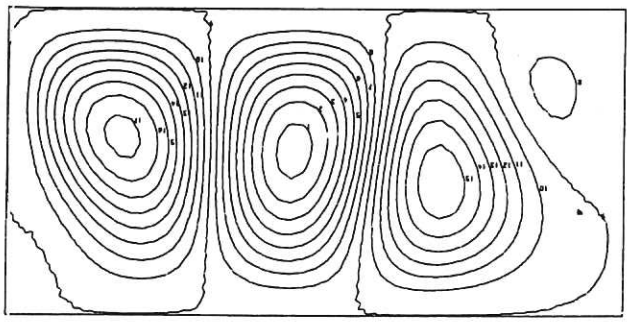

(b) Stream lines.
Stream function contour heights: 1 = - 8.0, 2 = - 7.0, 3 = - 6.0, 4 = - 5.0, 5 = - 4.0, 6 = - 3.0, 7 = - 2.0, 8 = - 1.0, 9 = 0.0, 10 = 1.0, 11 = 2.0, 12 = 3.0, 13 = 4.0, 14 = 5.0, 15 = 6.0, 16 = 7.0, 18 = 8.0.

Fig.3 Calculated contour plots for the case of Ralph and Roberts showing the initial surge of liquids. Ra = $5.0.10^5$, Pr = 5.39, Time = 0.0652.

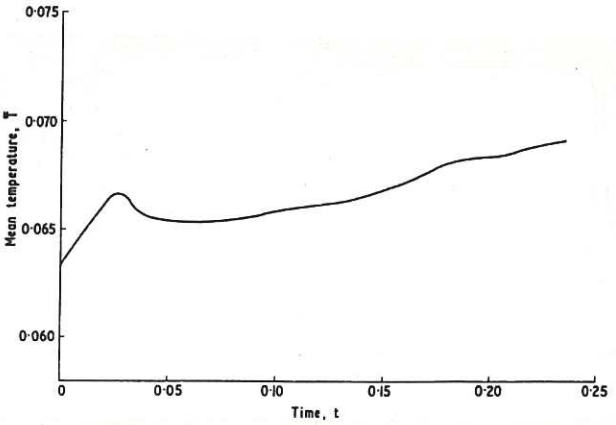

Fig.4 Calculated time variation of the mean temperature for the case of Ralph and Roberts. Ra = $5.0.10^6$, Pr = 5.39, width to height ratio = 2.

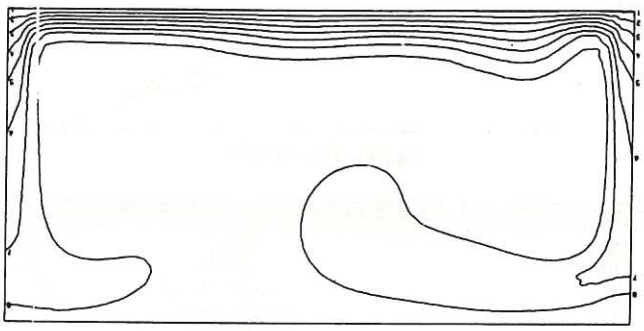

Fig.5(a) Time = 0.1659.

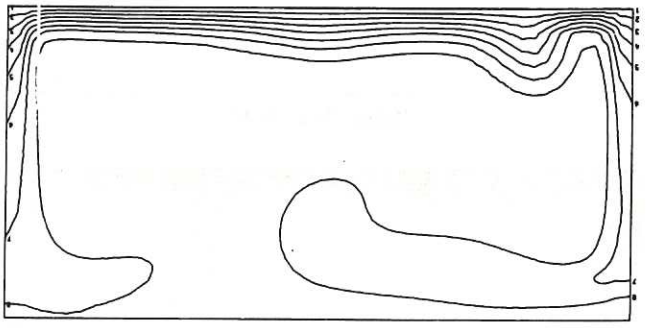

Fig.5(b) Time = 0.1707

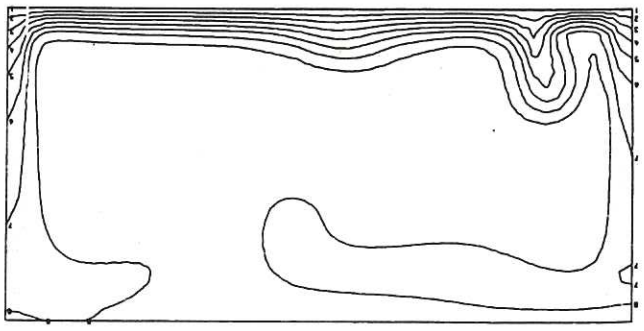

Fig.5(c) Time = 0.1755

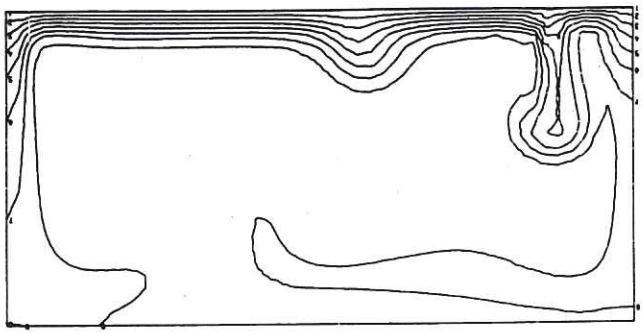

Fig.5(d) Time = 0.1803

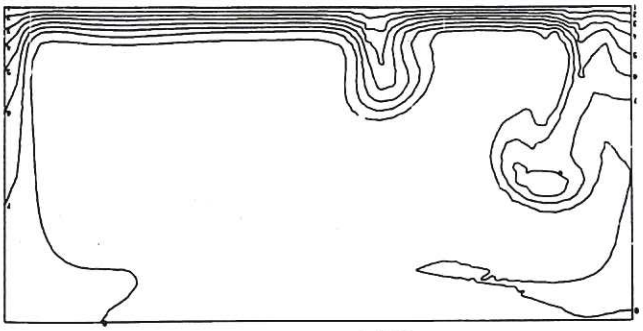

Fig.5(e) Time = 0.1851

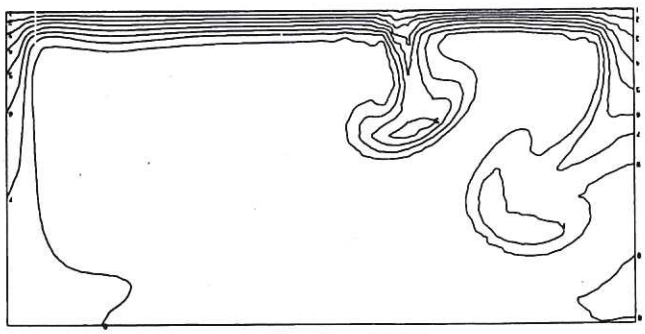

Fig.5(f) Time = 0.1899

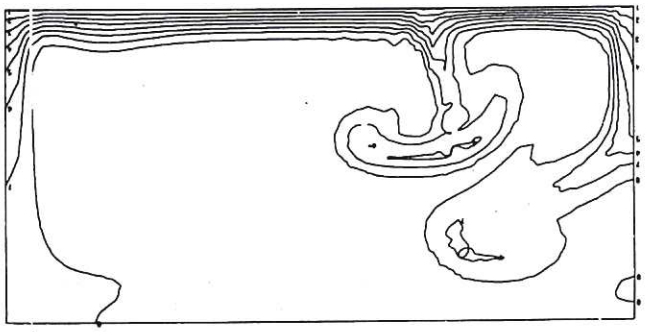

Fig.5(g) Time = 0.1947

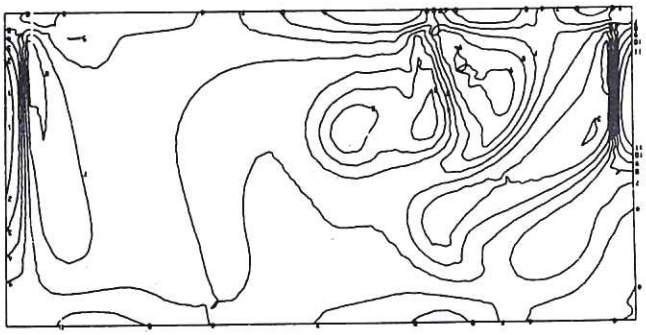

Fig.5(h) Contour plot of vorticity for Time = 0.1947
Vorticity contour heights: 1 = – 1000.0, 2 = – 800.0, 3 = – 600.0, 4 = – 400.0, 5 = – 200.0, 6 = 0.0, 7 = 200.0, 8 = 400.0, 9 = 600.0, 10 = 800.0, 11 = 1000.0.

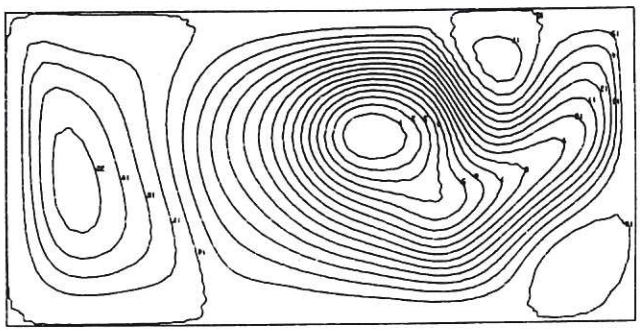

Fig.5(i) Stream lines for Time = 0.1947.
Stream function contour heights: 1 = – 15.0, 2 = – 14.0, 3 = – 13.0, 4 = – 12.0, 5 = – 11.0, 6 = – 10.0, 7 = – 9.0, 8 = – 8.0, 9 = – 7.0, 10 = – 6.0, 11 = – 5.0, 12 = – 4.0, 13 = – 3.0, 14 = – 2.0, 15 = – 1.0, 16 = 0.0, 17 = 1.0, 18 = 2.0, 19 = 3.0, 20 = 4.0.

Fig.5 Contour plots from calculation showing an intermittent jet of liquid from the cooled surface for the case of Ralph and Roberts. Ra = $5.0.10^6$, Pr = 5.39. Temperature contour heights: 1 = 0.0, 2 = 0.01, 3 = 0.02, 4 = 0.03, 5 = 0.04, 6 = 0.05, 7 = 0.06, 8 = 0.07.

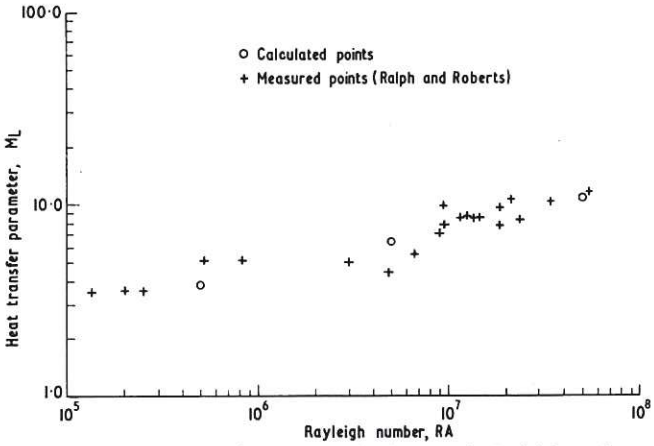

Fig.6 Plot of the heat transfer parameter (M_L) against the Rayleigh number (Ra) for the case of Ralph and Roberts showing calculated and measured values.

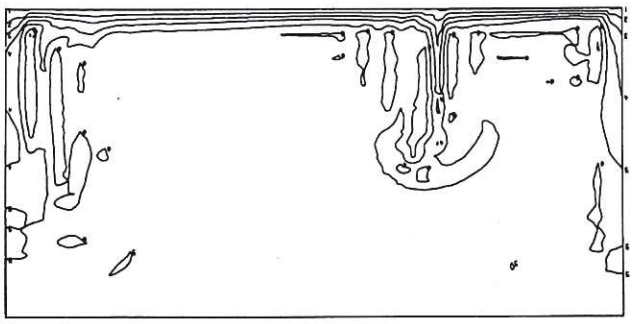

Fig.7(a) Mesh size 51 X 26.

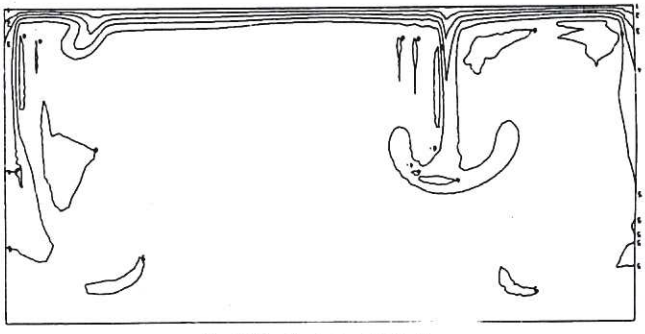

Fig.7(b) Mesh size 81 X 41.

Fig.7 Contour plots of the temperature for the case of Ralph and Roberts. Ra = $5.0.10^7$, Pr = 5.39, Time = 0.05655.

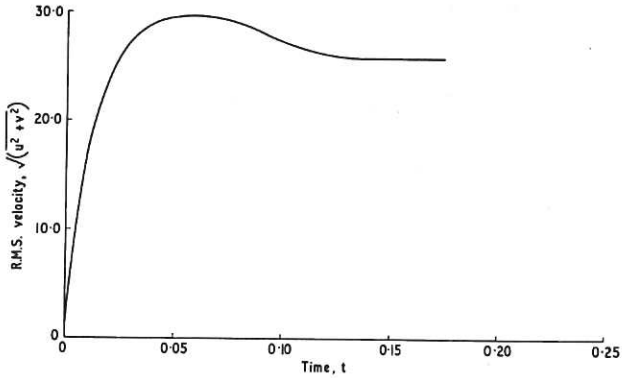

Fig.8 Calculated time variation of the root mean square velocity for the case of Wilkie and Fisher. Ra = $5.0.10^6$, Pr = 5.39, height to width ratio = 5.0.

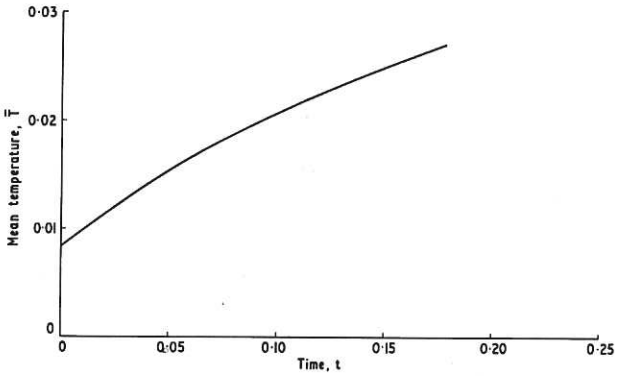

Fig.9 Calculated time variation of the mean temperature for the case of Wilkie and Fisher. Ra = $5.0.10^6$, Pr = 5.39, height to width ratio = 5.0.

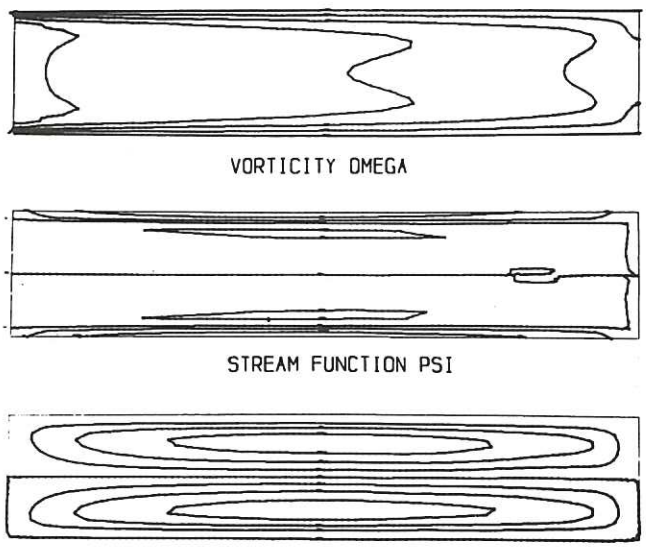

Fig.10 Contour plots from calculation for the case of Wilkie and Fisher. Ra = $5.0.10^6$, Pr = 5.39. Temperature contour heights: 1 = 0.0, 2 = 0.01, 3 = 0.02, 4 = 0.03, 5 = 0.04. Vorticity contour heights: 1 = – 800.0, 2 = – 400.0, 3 = 0.0, 4 = 400.0, 5 = 800.0. Stream function contour heights: 1 = – 6.0, 2 = – 4.0, 3 = – 2.0, 4 = 0.0, 5 = 2.0, 6 = 4.0, 7 = 6.0.